

Supporting information

Excess of Zn to Relieve the Structural Distortion of Manganese

Hexacyanoferrate in Aqueous Zn-ion Battery

Min Li ^[a, c], Mariam Maisuradze ^[a], Zulkarnaen Paputungan ^[a], Reinhard Denecke ^[b],
Jasper Rikkert Plaisier ^[c], Giuliana Aquilanti ^[c], Giovanni Agostini ^[c], Marco
Giorgetti ^{*[a]}

^[a] Department of Industrial Chemistry, University of Bologna, Campus Navile, Via Piero Gobetti
85, 40139 Bologna

^[b] Wilhelm-Ostwald-Institute of Physical and Theoretical Chemistry, Leipzig University, 04103
Leipzig, Germany

^[c] Elettra - Sincrotrone Trieste, s.s. 14, km 163.5, 34149, Trieste, Italy

* Corresponding Author: marco.giorgetti@unibo.it, phone: +39 051 2093 666

Experimental section

Synthesis of MnHCF, ZnHCF, and Zn-substituted MnHCF

The synthesis of MnHCF and ZnHCF has been reported in ref. ¹. The Zn-substituted MnHCF samples were synthesized in the same way as pure MnHCF. A series of solution A (100 mL ZnSO₄·7H₂O and MnSO₄·H₂O solutions mixed with different mole ratio, 0.005 M/0.095 M, 0.01 M/0.09 M and 0.035 M/0.065 M) were prepared, and added dropwise to an aqueous solution of sodium sulfate (Na₂SO₄, 0.1 M 100 mL), simultaneously with the solution B (100 ml 0.1 M sodium ferrocyanide decahydrate (Na₄Fe(CN)₆·10H₂O) solution), using a peristaltic pump at a rate of 4 mL min⁻¹. The reaction batch kept under N₂ atmosphere at a constant temperature (40 ± 2 °C) by using a water bath. The obtained solution was aged for five days, assuring complete decantation. Then, the precipitate was collected via centrifugation at 4000 rpm, washed three times with distilled water, and dried at 60 °C for 48 h.

Electrode preparation and electrochemical tests

The electrochemical test was conducted using 2032-coin cell: the active material as a working electrode, zinc sheet as reference and counter electrode. The working electrode was prepared by mixing the active material (70%), super C65 (25%) and PTFE (5%) and grinding, until a homogenous thin solid slice was obtained. Afterwards, a puncher was used to obtain 8 mm (diameter) pellets with a mass density of around 5~10 mg/cm². Cyclic voltammetry (CV) was performed by means of CH Instruments Model 660. The CV tests were conducted in potential range of 1.0-2.0 V vs Zn²⁺/Zn in 3 M ZnSO₄ aqueous solution. Galvanostatic cycling with potential limitation (GCPL) was conducted in 1.0 < E < 1.9 V vs Zn²⁺/Zn potential window at different current densities. Cycling started after a rest time (6 h) at OCP condition with a positive imposed current. All tests were performed at room temperature.

All the ex-situ electrodes were collected at 20 mA g⁻¹, the abbreviation C1 means the 1st Charge, and D1- the 1st Discharge. The same naming method is used for C2, D2, D10, D20, and D100.

Characterization

Microwave plasma-atomic emission spectrometer (MP-AES 4210, AGILENT) was used to detect the composition of the active material. During the test, three different wavelengths were chosen for each element.

Infrared (IR) spectrum was measured using a Bruker Alpha FT-IR spectrometer in ATR (Attenuated Total Reflectance) mode at a spectral range of 4000-400 cm^{-1} .

X-ray Photoelectron Spectroscopy (XPS) for the powder samples was performed with a VG ESCALAB 220 iXL spectrometer. The X-Ray source was non-monochromatized Al K α . During the experiment, the base pressure was 10^{-8} mbar. Detail spectra of relevant core levels were scanned four times at a pass energy of 50 eV with a step width of 0.1 eV and a dwell time of 300 ms. The detail spectra were corrected by subtraction of excitation satellites before peak fitting due to the non-monochromatized Al anode. Data analysis was performed by UNIFIT 2020 (<https://www.unifit-software.de/>). The background of the detail spectra was fitted using a combination of polynomial and Shirley background. Peaks shapes were simulated combining Lorentzian and Gaussian functions by convolution (Voigt profile). The binding energy scale was calibrated to the N 1s signal of cyanide to 397.6 eV.

XRD data were recorded by using a monochromatic X-ray beam (wavelength of 0.6199 Å) at the MCX beamline in ELETTRA synchrotron Trieste (Italy)². XRD data of the powder samples were collected in a capillary geometry, setting the spinner at 3000. Electrode samples were tested in transition mode with a marCCD detector. The XRD pattern was recorded consecutively in the range of $5^\circ < 2\theta < 70^\circ$, with a step of 0.01° and an acquisition time of 1 s step^{-1} . The XRD data are presented in Q index, which is independent from the wavelength. The Q is calculated by $4\pi \sin(\theta)/\lambda$, where θ is the Bragg angle, and λ is the X-ray wavelength. The crystal structure was refined using GSAS-II.

XAS experiments were conducted at Elettra Synchrotron Trieste (Italy), at the XAFS beamline³. Data were recorded at the Fe, Mn and Zn K-edge in transmission mode using ionization chambers filled with a mixture of Ar, N₂, and He to have 20, 70, and 95% of absorption in the I₀, I₁ and I₂ chambers, respectively. An internal reference of iron, manganese and zinc foil was used for the energy calibration in each scan. This allowed a continuous

monitoring of the energy during the consecutive scans. The white beam was monochromatized using a fixed exit monochromator equipped with a pair of Si (111) crystals. Spectra were collected from 6345 to 7100 eV, from 6920 to 8350 eV, and from 9467 to 10897 eV for Mn, Fe and Zn K-edges, respectively.

XAS data pretreatment was conducted using the Athena program ⁴, which includes the XANES normalization procedure. The pre-edge background was removed by subtraction of a linear function extrapolated from the pre-edge region, and the raw spectra were normalized to the unity by extrapolation of the atomic background evaluated using a polynomial function. XANES spectra were normalized to an edge jump of unity. A prior removal of the background absorption was done by subtraction of a linear function extrapolated from the pre-edge region. The EXAFS analysis was performed using the GNXAS package ⁵, which is based on multiple scattering (MS) theory. The method is based on the decomposition of the EXAFS signals into a sum of several contributions, the n-body terms. It allows the direct comparison of the raw experimental data with a model theoretical signal. The procedure avoids any filtering of the data and allows a statistical analysis of the results. EXAFS data analysis is performed by minimizing a χ^2 -like residual function that compares the theoretical signal to the experimental one.

- 1 M. Li, R. Sciacca, M. Maisuradze, G. Aquilanti, J. Plaisier, M. Berrettoni and M. Giorgetti, *Electrochim. Acta*, 2021, **400**, 139414.
- 2 J. R. Plaisier, L. Nodari, L. Gigli, E. P. R. S. Miguel, R. Bertocello and A. Lausi, *Acta IMEKO*, 2017, **6**, 71–75.
- 3 G. Aquilanti, M. Giorgetti, R. Dominko, L. Stievano, I. Arčon, N. Novello, L. Olivi, I. Ar, N. Novello, L. Olivi, I. Arčon, N. Novello and L. Olivi, *J. Phys. D: Appl. Phys.*, DOI:10.1088/1361-6463/aa519a.
- 4 M. Newville, DOI:10.1107/S0909049505012719.
- 5 A. Filipponi, A. Di Cicco and C. R. Natoli, *Phys. Rev. B*, 1995, **52**, 15122–15134.

Table S1. Chemical composition and cell parameters of MnHCF, ZnHCF, as well as the Zn-substituted MnHCF samples obtained from MP-AES and Pawley refinement results, respectively.

Samples	Chemical Composition	Space group	Pawley refinement					
			a (Å)	b(Å)	c(Å)	α (°)	β (°)	γ (°)
MnHCF	Na _{1.41} Mn [Fe (CN) ₆] _{0.89}	P21/n	10.867(2)	7.818(1)	7.618(2)	90	92.12(1)	90
3% ZnMnHCF	Na _{1.03} Zn _{0.03} Mn _{0.97} [Fe (CN) ₆] _{0.80}	Pm3m	5.127(4)	5.127(4)	5.127(4)	90	90	90
10% ZnMnHCF	Na _{0.95} Zn _{0.10} Mn _{0.90} [Fe (CN) ₆] _{0.78}	Pm3m	5.118 (1)	5.118 (1)	5.118 (1)	90	90	90
35% ZnMnHCF	Na _{0.84} Zn _{0.35} Mn _{0.65} [Fe (CN) ₆] _{0.76}	Pm3m	5.125(3)	5.125(3)	5.125(3)	90	90	90
		R-3c	12.159(2)	12.159(2)	31.973(3)	90	90	120
ZnHCF	K _{0.05} Zn [Fe (CN) ₆] _{0.77}	R-3c	12.554(3)	12.554(3)	33.019(2)	90	90	120

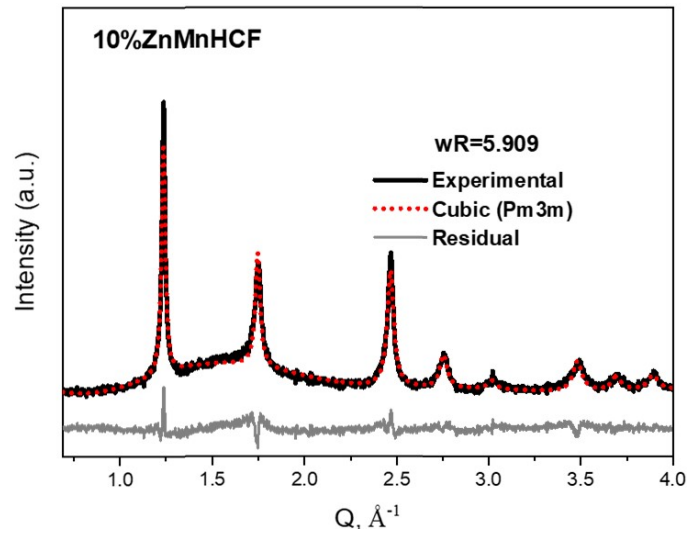


Figure S1. Pawley refinement of 10% ZnMnHCF XRD data with cubic (Pm3m) phase.

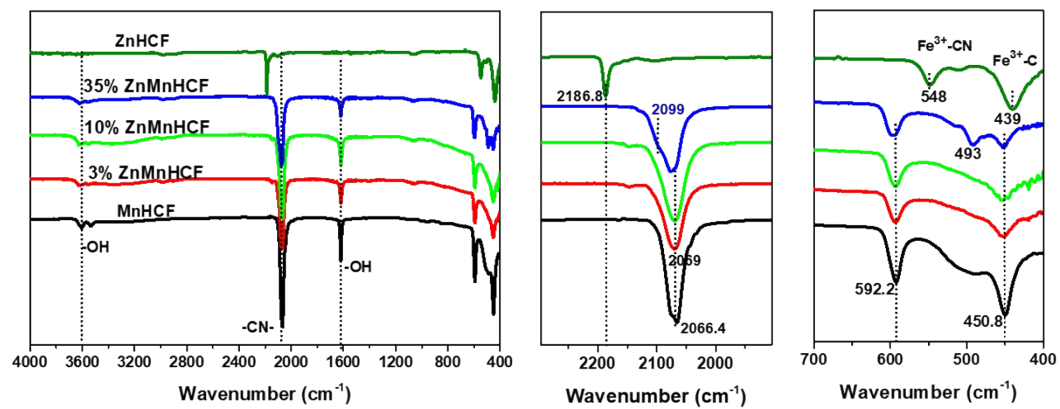


Figure S2. ATR-FTIR spectra of Zn-substituted MnHCF samples, MnHCF and ZnHCF powder samples, as well as the zoom-in of the $\nu(\text{CN})$ stretching and $\delta(\text{FeCN})$ bending & $\nu(\text{FeC})$ stretching band;

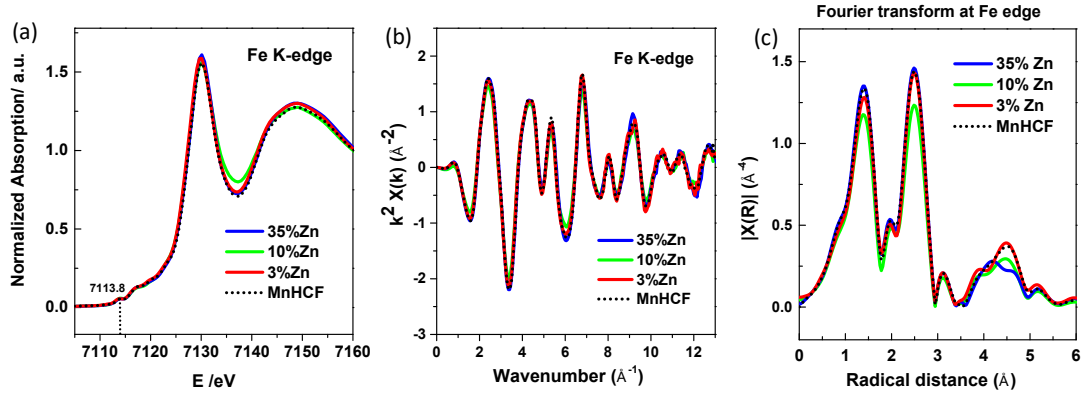


Figure S3. XANES spectra of (a) Fe K-edge of Zn-substituted MnHCF samples; k^2 -weighted EXAFS signals of (b) Fe K-edge, as well as the (c) corresponding Fourier transform (FT) of k^2 -weighted EXAFS signal.

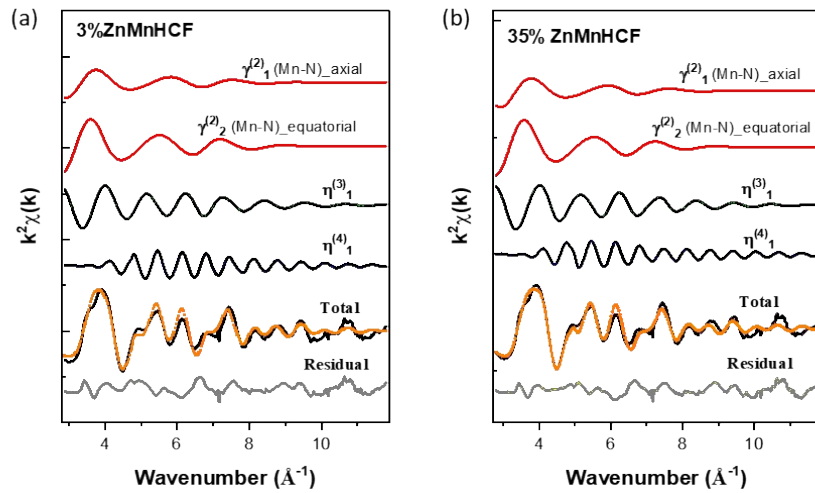


Figure S4. EXAFS analysis of Mn K-edge of (d) 3% ZnMnHCF and (e) 35% ZnMnHCF samples, each panel of the figure shows the individual EXAFS contributions, in terms of two-body, three-body and four-body signals, to the total theoretical signal.

Table S2. EXAFS fitting parameters for Mn K-edge.

	MnHCF	3% ZnMnHCF	10% ZnMnHCF	35% ZnMnHCF
Mn- N / Å σ^2 Mn-N / Å ²	2.198(3) ^a 0.007(6)	2.170(1) ^b 0.005(8)	2.158(4) ^b 0.015	2.146(8) ^b 0.003(7)
Mn- N / Å σ^2 Mn-N / Å ²	-	2.279(4) ^c 0.010(8)	2.254(7) ^c 0.014(5)	2.258 ^c 0.011(5)
C- N / Å σ^2 C-N / Å ²	1.160 0.003(8)	1.189(9) 0.006(3)	1.199(9) 0.001(8)	1.189(9) 0.011(3)
C- Fe / Å σ^2 C-Fe / Å ²	1.852(3) 0.014(3)	1.878(6) 0.011(8)	1.887(2) 0.004(5)	1.875(4) 0.011(9)
θ Mn-N-C / deg	175	175	175	175
E ₀ Mn / eV	6551.7	6551.5	6550.8	6551.5
R residual / (10 ⁻⁶)	6.06	4.40	3.95	3.03

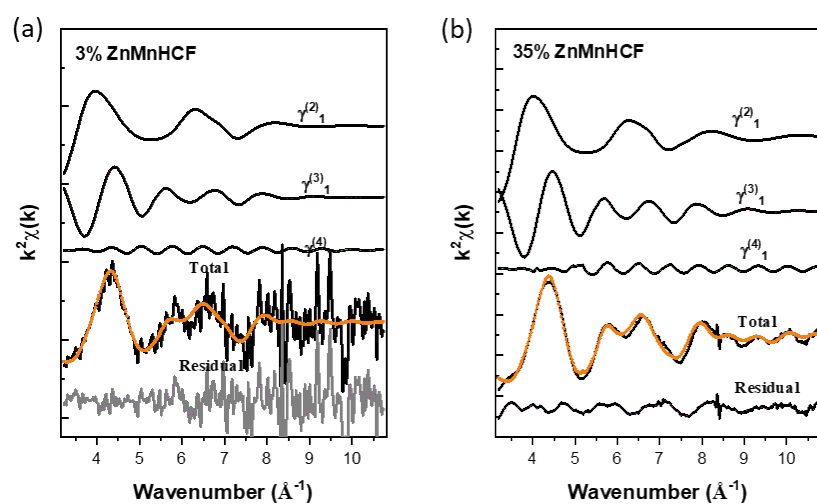
^aCN=6. ^bCN=2. ^cCN=4**Figure S5.** EXAFS analysis of Zn K-edge of (a) 3% ZnMnHCF and (b) 35% ZnMnHCF samples

Table S3. EXAFS fitting parameters for Zn K-edge.

	ZnHCF	3% ZnMnHCF	10% ZnMnHCF	35% ZnMnHCF
Zn- N / Å σ^2 Mn-N / Å ²	1.963 0.010(5)	1.951(6) 0.014	1.924 0.006(1)	1.942(3) 0.004(3)
C- N / Å σ^2 C-N / Å ²	1.101 0.006(5)	1.125(8) 0.002(2)	1.124(5) 0.008(7)	1.116(4) 0.012(2)
C- Fe/ Å σ^2 C-Fe / Å ²	1.914(5) 0.012(6)	1.800 0.004(7)	1.800 0.001	1.884(4) 0.007(9)
θ Zn-N-C / deg	170	170	170	170
E_0 Zn / eV	9664.5	9661.2	9661.6	9661.8
R residual / (10 ⁻⁶)	1.97	12.7	4.13	4.24

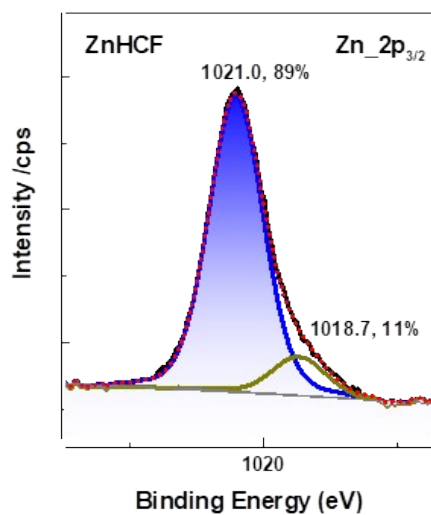


Figure S6. Zn 2p_{3/2} XPS data of ZnHCF.

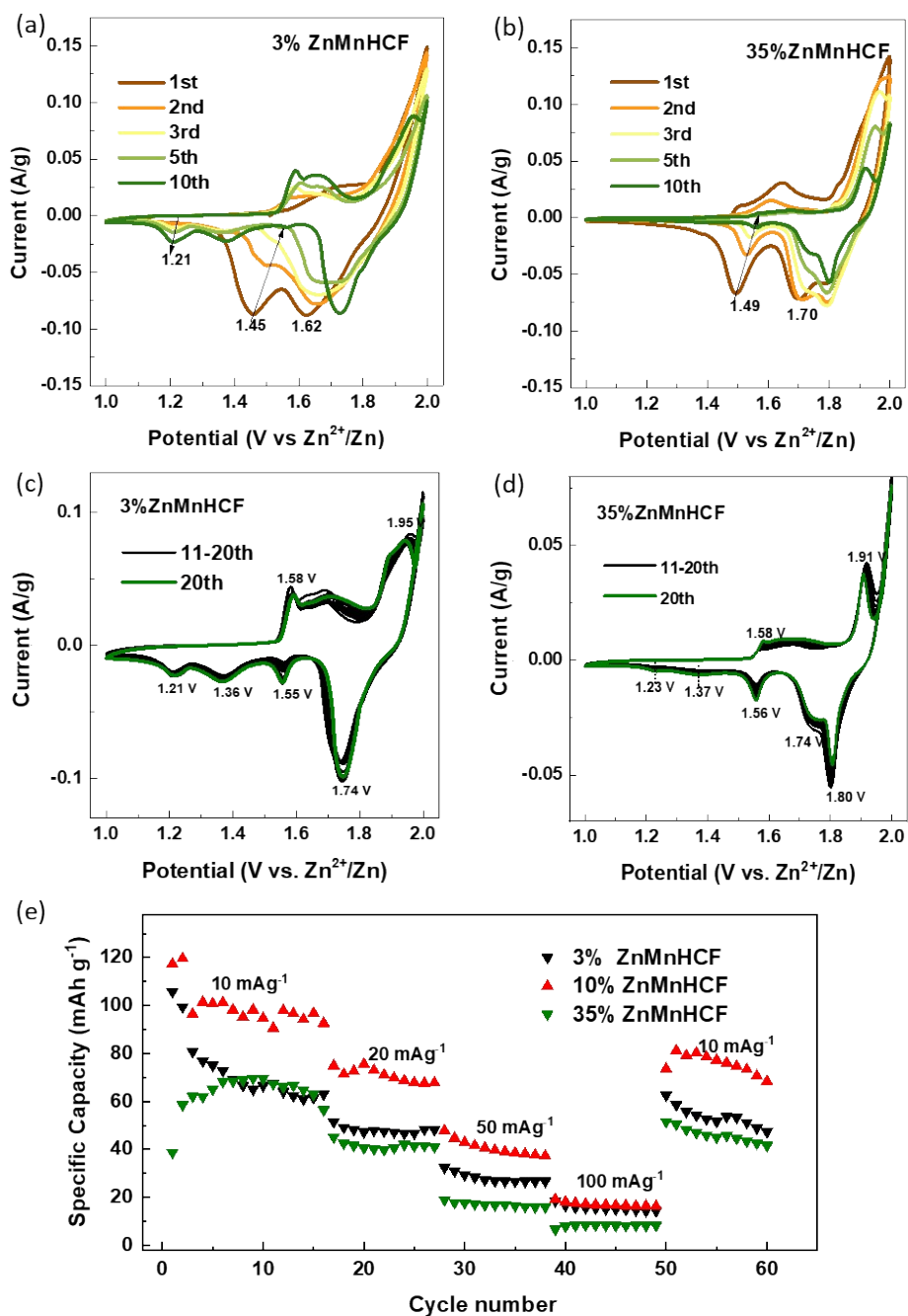


Figure S7. CV data of (a, c) 3% ZnMnHCF, (b, d) 35% ZnMnHCF in 3M ZnSO₄ electrolyte at 0.2 mV/s for 20 cycles; (e) rate capability data of Zn-substituted MnHCF samples.

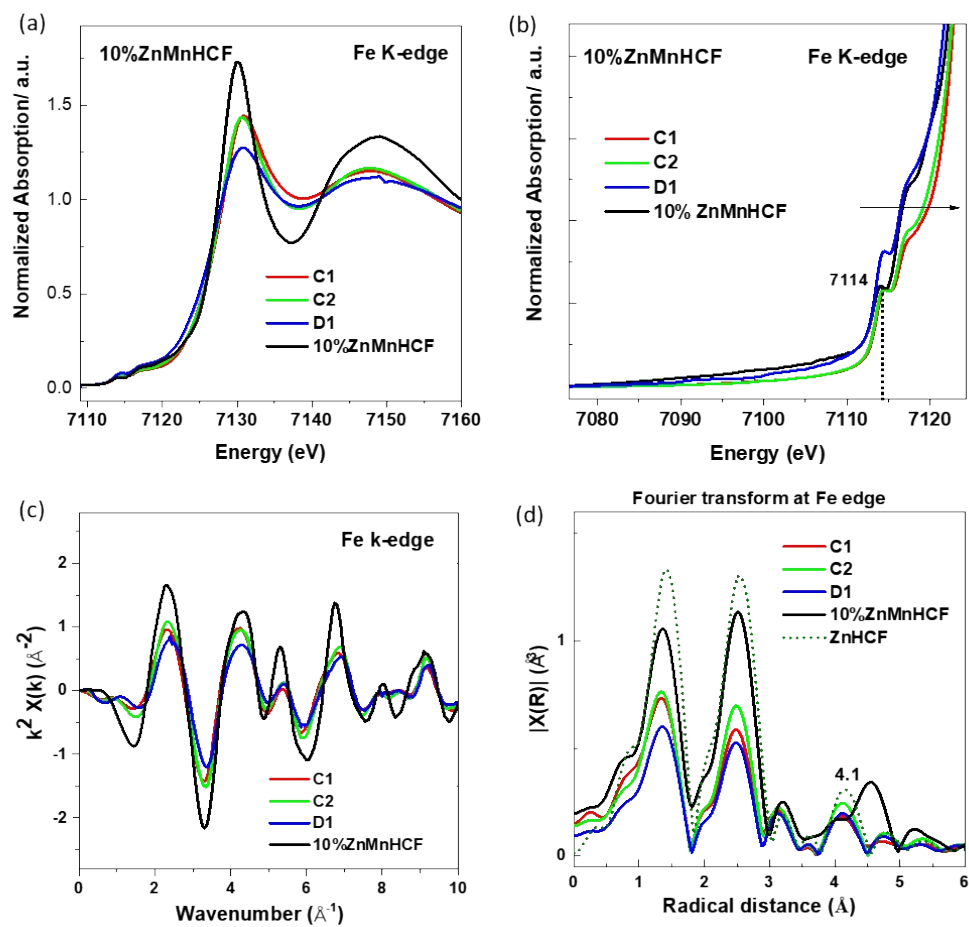


Figure S8. (a) Ex-situ XANES of Fe K-edge at different charge/discharge states (C1, D1 and C2 states); (b) zoom-in of the pre-edge region; (c) k^2 -weighted EXAFS signals and (d) corresponding Fourier transform (FT) of Mn k^2 -weighted EXAFS signal.

Table S4. EXAFS fitting parameters for Fe K-edge.

	10% ZnMnHCF	10% ZnMnHCF_C1	10% ZnMnHCF_D1	10% ZnMnHCF_C2
Fe- C / Å σ^2 Mn-N / Å ²	1.897 0.007(7)	1.936(1) 0.012(3)	1.913(9) 0.014(5)	1.921(3) 0.012(2)
C- N / Å σ^2 C-N / Å ²	1.142(4) 0.006(2)	1.101(4) 0.004(71)	1.109(5) 0.003(6)	1.104(3) 0.002(7)
N- Mn / Å σ^2 C-Fe / Å ²	2.197(4) 0.010	2.244(4) 0.009(9)	2.255(7) 0.009(8)	2.255(1) 0.009(9)
θ Mn-N-C / deg	175	175	175	175
E ₀ Mn / eV	7127.9	7128.0	7127.2	7127.8
R residual / (10 ⁻⁶)	4.06	3.07	1.68	3.39

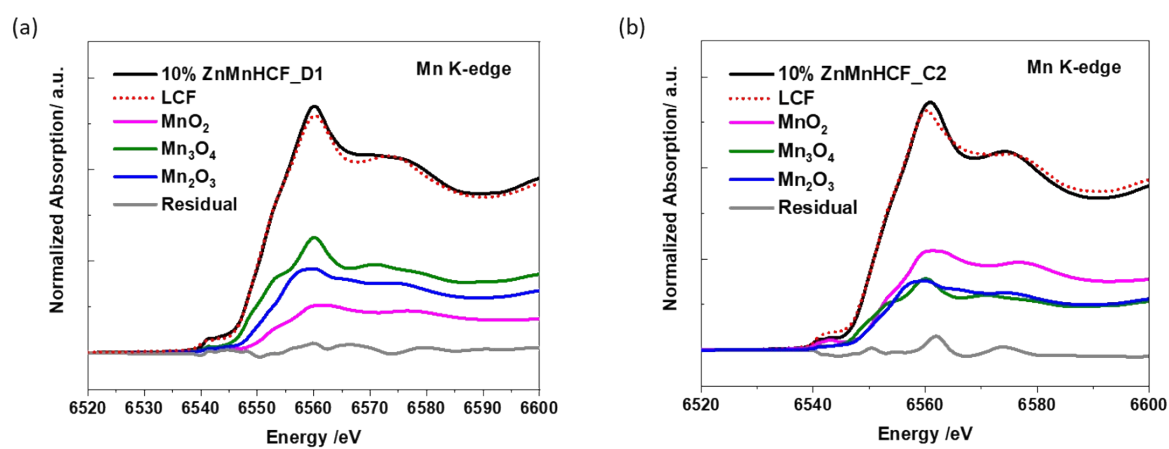


Figure S9. Linear combination fitting of the normalized XANES spectra of 10% ZnMnHCF_D1 and 10% ZnMnHCF_C2 electrodes.

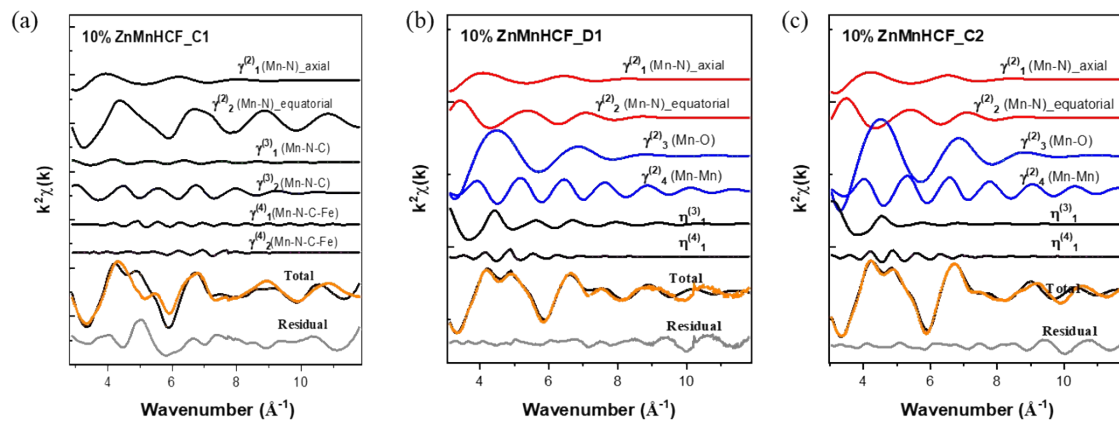


Figure S10. (a) EXAFS fitting results of 10% ZnMnHCF_C1 based on one model (MnHCF model); EXAFS of Mn K-edge fitting results based on two models for (b) 10% ZnMnHCF_D1 and (c) 10% ZnMnHCF_C2 electrodes.

Table S5. EXAFS fitting parameters for Mn K-edge.

	10% ZnMnHCF	10% ZnMnHCF_C1	10% ZnMnHCF_D1	10% ZnMnHCF_C2
^a Mn- N / Å σ^2 Mn-N / Å ²	2.158(4) 0.015	1.945(5) 0.014(9)	1.978(7) 0.0150	1.964(2) 0.006(7)
^b Mn- N / Å σ^2 Mn-N / Å ²	2.254(7) 0.014(5)	2.279(9) 0.011(6)	2.279(9) 0.012(3)	2.279(9) 0.012
Mn- O / Å σ^2 Mn-N / Å ²	-	1.859(1) 0.013(9)	1.887(2) 0.013(5)	1.856(7) 0.012(3)
Mn- Mn / Å σ^2 Mn-N / Å ²	-	2.975(9) 0.011(9)	2.977 0.012(8)	2.950(6) 0.012
C- N / Å σ^2 C-N / Å ²	1.199(9) 0.001(8)	1.167(1) 0.015	1.108(5) 0.0149(9)	1.150(7) 0.014(9)
C- Fe / Å σ^2 C-Fe / Å ²	1.887(2) 0.004(5)	1.997(5) 0.007(6)	2.045(5) 0.012(1)	1.961(9) 0.012
θ Mn-N-C / deg	175	175	175	175
E ₀ Mn / eV	6550.8	6550.4	6548.1	6549.9
R residual / (10 ⁻⁶)	3.95	4.26	1.07	2.46

* ^aCN=2. ^bCN=4.

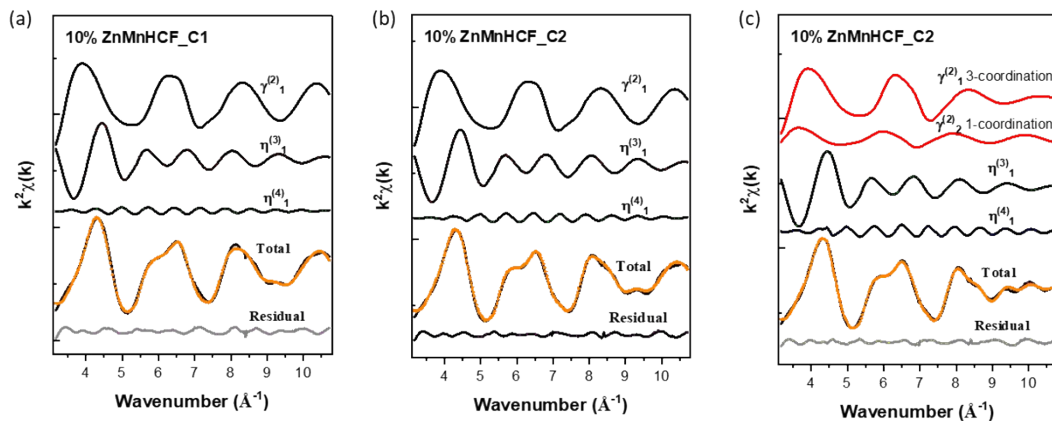


Figure S11. EXAFS fitting results of (a) 10% ZnMnHCF_C1 electrode and (b) 10% ZnMnHCF_C2 electrode based on ZnN₄ model and (c) 10% ZnMnHCF_C2 electrode based on ZnN₃O model.

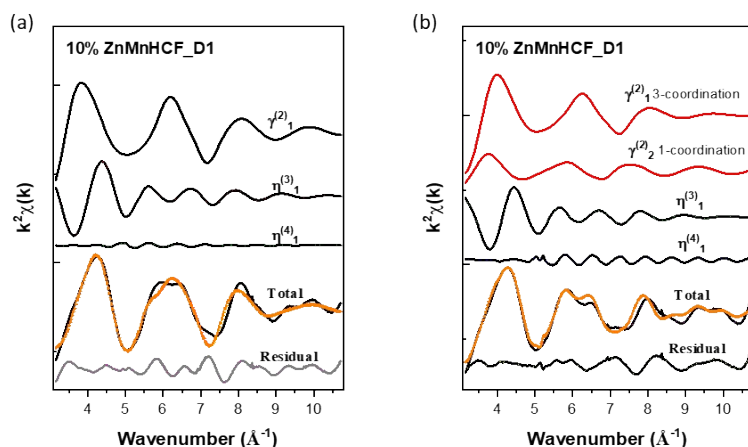


Figure S12. EXAFS fitting results of (a) 10% ZnMnHCF_D1 based on ZnN₄ model and (b) 10% ZnMnHCF_D1 electrode based on ZnN₃O model.

Table S6. EXAFS fitting parameters for Zn K-edge.

	10% ZnMnHCF (tetrahedral)	10% ZnMnHCF_C1 (tetrahedral)	10% ZnMnHCF_C1 (distorted tetrahedral)	10% ZnMnHCF_C2 (tetrahedral)	10% ZnMnHCF_C2 (distorted tetrahedral)	10% ZnMnHCF_D1 (tetrahedral)	10% ZnMnHCF_D1 (distorted tetrahedral)	10% ZnMnHCF_D1 (octahedral)	10% ZnMnHCF_D2 (octahedral)	10% ZnMnHCF_D20 (distorted tetrahedral)
Zn- N / Å σ^2 Mn-N / Å ²	1.924 0.006(1)	1.963(9) 0.003(7)	1.933(4) ^a 0.006(3)	1.961(8) 0.003(7)	1.934(9) ^a 0.004(3)	1.988(6) 0.006 (4)	2.036(7) ^a 0.010(5)	1.930(9) ^c 0.009(4)	1.929(7) ^c 0.005 (3)	1.942(3) ^a 0.013 (5)
Zn- O / Å σ^2 Mn-N / Å ²	-	-	2.064(3) ^b 0.002	-	2.028(5) ^b 0.004	-	2.146(3) ^b 0.003(9)	2.078 ^d 0.002	2.065(5) ^d 0.0020	2.035(4) ^b 0.002
C- N / Å σ^2 C-N / Å ²	1.124(5) 0.008(7)	1.058(9) 0.0090	1.100 0.013(2)	1.052(3) 0.007(5)	1.055(3) 0.005(5)	1.066(2) 0.005(6)	1.095(6) 0.003(7)	1.100 0.014	1.127(8) 0.006(8)	1.133(7) 0.006(1)
C- Fe / Å σ^2 C-Fe / Å ²	1.800 0.001	1.850(1) 0.001(4)	1.814(4) 0.005(6)	1.857(3) 0.005(4)	1.838(5) 0.007(5)	1.880 0.006(5)	1.800 0.009(5)	1.818 0.001	1.800 0.0010	1.835(8) 0.001(3)
θ Mn-N-C / deg	170	170	170	170	170	170	170	170	170	170
E ₀ Mn / eV	9661.6	9662.0	9662.0	9662.0	9662.0	9662.5	9662.5	9662.5	9661.5	9660.9
R residual / (10 ⁻⁶)	4.13	4.89	4.52	3.59	3.28	24.5	12.9	5.76	1.17	5.19

*

^aCN=3.

^bCN=1;

^cCN=4.

^dCN=2

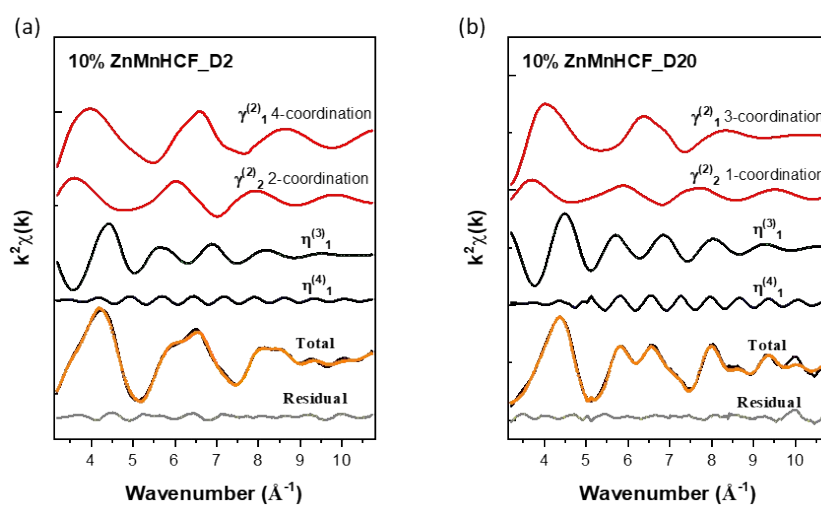


Figure S13. (a) EXAFS fitting results at Zn K-edge for (a) 10% ZnMnHCF_D2 based on ZnN_4O_2 model and (b) 10% ZnMnHCF_D20 electrodes based on ZnN_3O model.